ISSN 1392–1207. MECHANIKA. 2022 Volume 28(3): 217–221

Multiscale Analysis of the Performance of Micro/nano Porous Filtration Membranes with Double Concentric Cylindrical Pores: Part II-Optimization Results

Zhipeng TANG*, Yongbin ZHANG**
**College of Mechanical Engineering, Changzhou Vocational Institute of Mechatronic Technology, Changzhou, Jiangsu Province, China, E-mail: tzp2192@czimt.edu.cn*
***College of Mechanical Engineering, Changzhou University, Changzhou, Jiangsu Province, China, E-mail: yongbinzhang@cczu.edu.cn; engmech1@sina.com (Corresponding Author)*
crossref http://dx.doi.org/10.5755/j02.mech.30509

1. Introduction

Nano porous filtration membranes have important applications in super purification, desalination, hemofiltration, DNA analysis, drug delivery, and bisosensors etc. [1-9]. Their advantage is to use the very small filtration pore with the nanometer scale radius. Consequently, one of their shortcomings is the much-reduced flux. When the radius of the filtration pore is so small that the flowing liquid across the pore radius all become non-continuum, the flow equation for nanoscale flow can solely solve the flow problem in the membranes [10]. However, when the membrane is used to separate the particles with relatively big size such as the impurities, bacteria, virus and organic macro molecules, the radius of the filtration pore may be relatively large such as on the scales of 10nm and even 100nm, the flowing liquid through the membrane may be mainly continuum inside the pores, but the adhering layer on the pore wall may have a considerable effect on the flux of the membrane owing to its thickness comparable to the pore radius. For this case, the multiscale approach is required for analyzing the flow and flux of the membrane by simultaneously incorporating the flows of the adsorbed layer and the continuum liquid.

The studies on nanoporous filtration membranes were mainly experimental with emphasis on their manufacturing [1, 2, 5-7, 11-14]. Theoretical researches on them are scarce mainly because of the difficulty in simulating the nanoscale flow in an engineering problem caused by molecular dynamics simulation (MDS) [15, 16]. When facing the multiscale flow in the membrane, the challenging in the simulation problem exists the same owing to using MDS to simulate the adsorbed layer flow [17, 18].

In the first part [19], we presented the multiscale analysis results for the flow resistance of the nanoporous filtration membrane where multiscale flow occurs, by using the flow equation for nanoscale flow to simulate the adsorbed layer flow and using the fluid Newtonian model to simulate the continuum liquid flow. The advantage of the present multiscale analysis is to give the fast results directly by inputting the parameter values. For improving the flux, in the studied membrane is also designed the bigger flow resistance-reducing pore, where may also occur the multiscale flow. We have noticed the best ratio of the radius of the bigger pore to the radius of the filtration pore which gives the maximum flux of the membrane. The present study is the successive work of the first part. In the present paper, we present the detailed optimization analysis and calculation for the studied membrane, and compare the obtained results from the multiscale analysis with the classical theory calculations. Important conclusions have been obtained regarding how to optimize the studied membrane from the viewpoint of the multiscale flow.

2. Studied membrane

The studied membrane has been shown in the first part [19]. Here, for easy understanding, it is shown again in Figs. 1a and b. There are two concentric cylindrical pores across the membrane thickness, one is smaller with the radius R_0 and for filtration, and the other is bigger with the radius R_1 ($R_1 > R_0$) and for reducing the flow resistance. The axial lengths of the two pores and the membrane thickness are respectively l_0, l_1 and l. As shown in Fig. 1b, the radius of the filtration pore is so large that near the pore wall occurs the flow of the adsorbed layer with the layer thickness h_{bf} and in the central region of the pore occurs the continuum liquid flow. Both of these two flows may significantly contribute to the flux of the membrane.

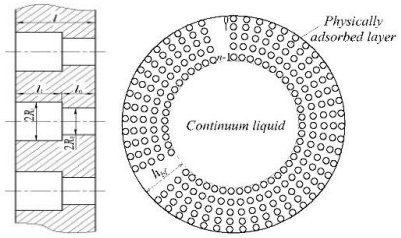

a b

Fig. 1 The studied nanoporous filtration membrane with multiscale flow. a) The membrane profile; b) Flowing media inside the magnified filtration pore [19]

3. Analysis

3.1. Multiscale analysis

The multiscale analysis for the multiscale flow in the studied membrane has been shown in the first part [19], by neglecting the interfacial slippage on any interface. Here, for brevity, the detailed derivation and analytical results for the present membrane are not repeated.

3.2. Classical analysis

The classical analysis for the liquid flow in the

membrane neglected both the adsorbed layer on the pore wall and any interfacial slippage and assumed the whole liquid as continuum whenever the pore radius is small or large. It calculates the dimensionless flow resistance of the membrane from the following equation [10]:

$$F_{conv}\left(\frac{R_1}{R_0}\right)=\lambda_0\left(\frac{R_1}{R_0}\right)^2+(1-\lambda_0)\left(\frac{R_0}{R_1}\right)^2, \quad (1)$$

where: F measures the dimensionless flow resistance of the membrane and was defined in the first part (by Eq. (8)), and $\lambda_0 = l_0/l$.

The classical analysis gives the following optimum value of R_1/R_0 for the maximum flux of the membrane [10]:

$$\left(\frac{R_1}{R_0}\right)_{opt}=\left(\frac{1-\lambda_0}{\lambda_0}\right)^{\frac{1}{4}}. \quad (2)$$

It gives the following equation for calculating the correspondingly resulting lowest flow resistance of the membrane when R_1/R_0 is optimum [10]:

$$F_{min}=2\sqrt{\lambda_0(1-\lambda_0)}. \quad (3)$$

4. Results

The calculations were made for the dimensionless flow resistances of the membrane, the optimum values of R_1/R_0 and the corresponding lowest dimensionless flow resistance of the membrane by using the present multiscale scheme when the liquid-pore wall interaction is respectively weak, medium-level and strong. These calculations were respectively compared with those calculated from the classical analysis (Eqs. (1-3) for the same operating conditions.

In the present calculations, $\Delta x / D = \Delta_{n-2} /$ $/D = 0.15$ and $\eta_{line,i} / \eta_{line,i+1} = q_0^m$, where q_0 and m are respectively positive constant [19] (The detailed definitions of all these symbols are shown in the first part).

In the present multiscale calculation, it is formulated that [10, 19]:

$$\frac{\eta_{bf}^{eff}}{\eta}=C_y(H_{bf})=a_0+\frac{a_1}{H_{bf}}+\frac{a_2}{H_{bf}^2}, \quad (4)$$

where: η_{bf}^{eff} is the effective viscosity of the adsorbed layer across the layer thickness; η is the bulk viscosity of the liquid flowing through the membrane; $H_{bf} = h_{bf} / h_{cr,bf}$, $h_{cr,bf}$ is a critical thickness; a_0, a_1 and a_2 are respectively constant.

It is formulated that [10, 19]:

$$\frac{\rho_{bf}^{eff}}{\rho}=C_q(H_{bf})=m_0+m_1H_{bf}+m_2H_{bf}^2+m_3H_{bf}^3, \quad (5)$$

where: ρ_{bf}^{eff} is the average density of the adsorbed layer; ρ is the bulk density of the flowing liquid; m_0, m_1, m_2 and m_3 are respectively constant.

The equations for calculating the important parameters ε, F_1 and F_2 in the present multiscale analysis have been shown in the first part [19] and here are not repeated.

The weak, medium and strong liquid-pore wall interactions respectively have the following parameter values:

Weak interaction: m = 0.5; n = 3; q_0 = 1.03; $h_{cr,bf}$ = 7 nm.

Medium interaction: m = 1.0; n = 5; q_0 = 1.1; $h_{cr,bf}$ = 20 nm.

Strong interaction: m = 1.5; n = 8; q_0 = 1.2; $h_{cr,bf}$ = 40 nm.

The other input parameter values are shown in Tables 1 and 2.

Table 1

Liquid viscosity data for different liquid-pore wall interactions [10, 19]

Parameter / Interaction	a_0	a_1	a_2
Strong	1.8335	-1.4252	0.5917
Medium	1.0822	-0.1758	0.0936
Weak	0.9507	0.0492	1.6447×10^{-4}

Table 2

Liquid density data for different liquid-pore wall interactions [10, 19]

Parameter / Interaction	m_0	m_1	m_2	m_3
Strong	1.43	-1.723	2.641	-1.347
Medium	1.30	-1.065	1.336	-0.571
Weak	1.116	-0.328	0.253	-0.041

4.1. Comparison of the calculated flow resistance with the classical calculation

Figs. 2, a-c respectively show the dimensionless flow resistances F of the present membrane calculated from the multiscale analysis for the weak, medium and strong liquid-pore wall interactions and their comparisons with those F_{conv} calculated from the classical flow theory (Eq. (1)). For $\lambda_x \geq 0.1$, the values of F are obviously greater than those of F_{conv} for the same operating conditions for all the types of liquid-pore wall interactions. This indicates the pronounced effect of the adsorbed layer in the multiscale flow which impedes the liquid flow through and reduces the flux of the membrane. The classical flow theory would overestimate the flux of the membrane particularly for $\lambda_x \geq 0.1$ and for the medium and strong liquid-pore wall interactions. It was found that with the increase of λ_x or/and with the increased liquid-pore wall interaction strength, the errors of the classical calculation of the flow resistance as compared to the multiscale calculation are significantly increased; It shows the increasing effect of the adsorbed layer. The results show that when $\lambda_x \geq 0.1$, the multiscale calculation may usually be mandatory for the flux of the membrane, and the membrane design should be based on the multiscale flow theory.

All these figures show that there are the optimum values of R_1/R_0 which give the smallest flow resistances and thus the highest fluxes of the membrane whenever calculated by the present multiscale scheme or by the clas-

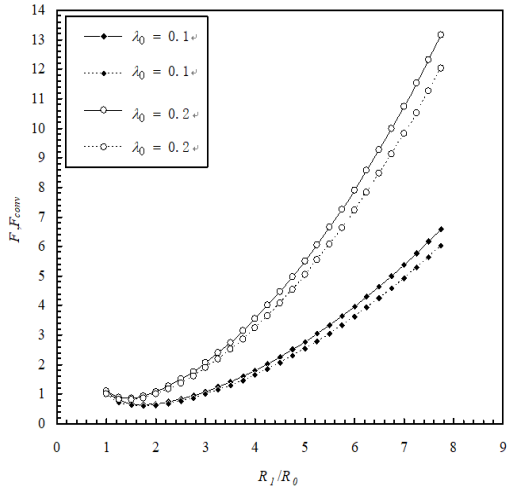

a) Weak interaction

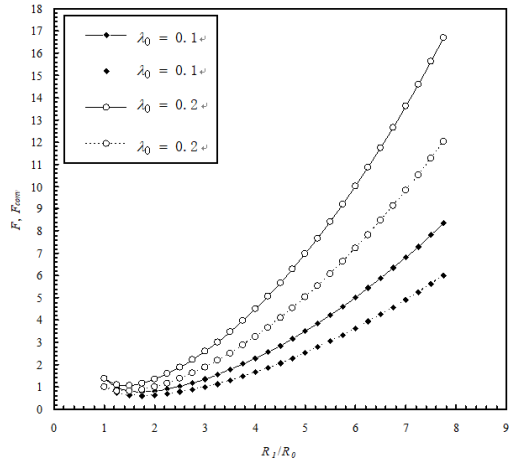

b) Medium interaction

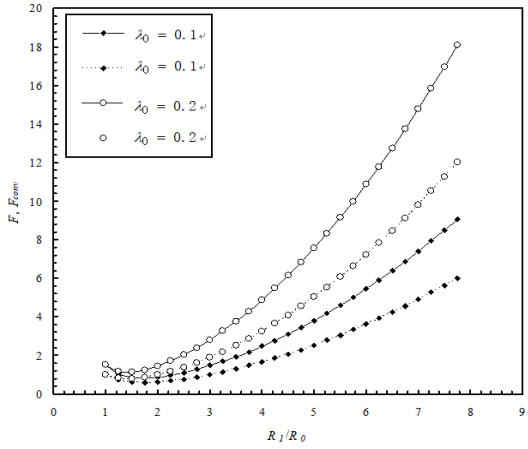

c) Strong interaction

Fig. 2 Dimensionless flow resistances of the present membrane calculated from the multiscale analysis respectively for the weak, medium and strong liquid-pore wall interactions when λ_x = 0.1 and their comparisons with those calculated from the classical equation (Eq. (1)) for the same cases. Solid line denotes the present multiscale calculation result F, and dashed line denotes the classical calculation F_{conv}

sical flow theory. For the optimum value of R_1/R_0, the discrepancy of the classical calculation from the multiscale calculation appears the smallest. The multiscale calculation results in the figures show that the ratio R_1/R_0 should be designed as the optimum value for achieving the lowest flow resistance of the membrane especially for the medium and strong liquid-pore wall interactions owing to the adsorbed layer effect.

4.2. Comparison of the calculated optimum value of R_1/R_0 with the classical calculation

Figs. 3, a-c show the optimum values ($(R_1/R_0)_{opt}$)

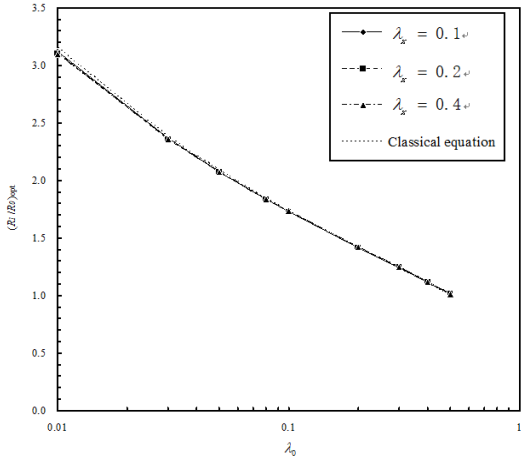

a) Weak interaction

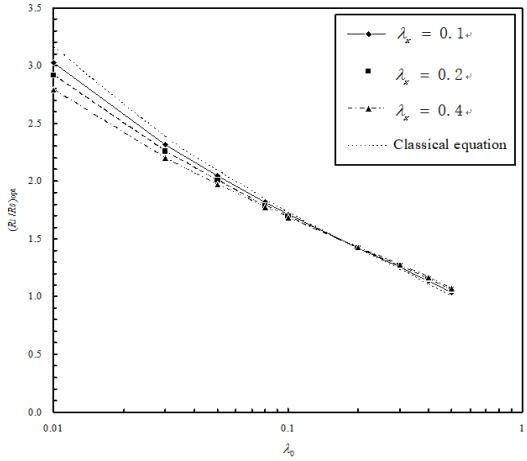

b) Medium interaction

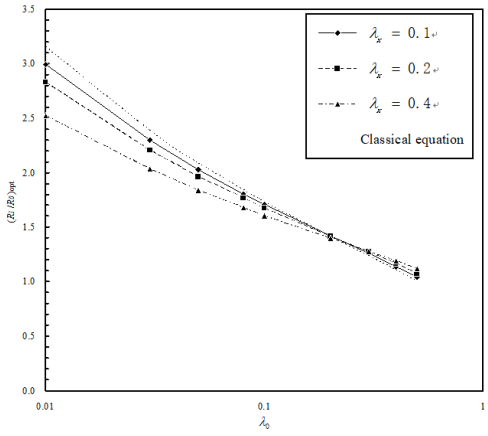

c) Strong interaction

Fig. 3 The optimum values ($(R_1/R_0)_{opt}$) of R_1/R_0 for the lowest flow resistance of the membrane calculated from the multiscale analysis and their comparisons with those calculated from the classical equation (Eq. (2))

of R_1/R_0 for the lowest flow resistance of the membrane calculated from the multiscale analysis when the liquid-pore wall interaction is respectively weak, medium and strong; The calculations are also compared with those by the classical equation (Eq. (2)). For the weak liquid-pore wall interaction, the values of $(R_1/R_0)_{opt}$) calculated from the multiscale analysis are very close to those calculated by the classical equation for the practical values of λ_x and λ_0. For the medium liquid-pore wall interaction, only when $\lambda_x \geq 0.1$, the present multiscale calculation is close to the classical calculation; Otherwise, it is lower than the classical calculation especially for greater values of λ_x, showing the significant multiscale effect owing to the adsorbed layer. For the strong liquid- pore wall interaction, when λ_0 = =0.2, the present multiscale calculation is close to the classical calculation.

When $\lambda_0 < 0.2$, it is lower than the classical calculation; While for $\lambda_0 > 0.2$, it is higher than the classical calculation. The figures show the significant multiscale influence on the value of $(R_1/R_0)_{opt}$) which is stronger for greater values of λ_x and stronger liquid-pore wall interactions. The results strongly indicate that the value of $(R_1/R_0)_{opt}$ should be calculated from the multiscale scheme when $\lambda_x \geq 0.1$ and the liquid-pore wall interaction is medium or strong; Nevertheless, for a weak liquid-pore wall interaction, the value of $(R_1/R_0)_{opt}$) can still be calculated from the classical equation.

4.3. Comparison of the calculated lowest flow resistance of the membrane with the classical calculation

Figs. 4, a-c show the dimensionless lowest flow resistances of the membrane calculated from the present multiscale analysis when the values of R_1/R_0 are optimum, respectively for the weak, medium and strong liquid-pore wall interactions; The calculations are also compared with those from the classical equation (Eq. (3)). It is shown that when $\lambda_x \geq 0.1$, for the same operating condition, the lowest flow resistance of the membrane calculated from the multiscale analysis is considerably higher than the classical calculation even for the weak liquid-pore wall interaction; When the liquid-pore wall interaction is medium or strong, the present multiscale calculation is much greater than the classical calculation especially for large λ_0 values.

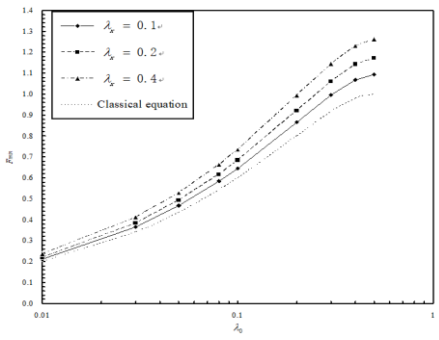

a) Weak interaction

Fig. 4 The dimensionless lowest flow resistances of the membrane calculated from the multiscale analysis when the values of R_1/R_0 are optimum, and their comparisons with those calculated from the classical equation (Eq. (3))

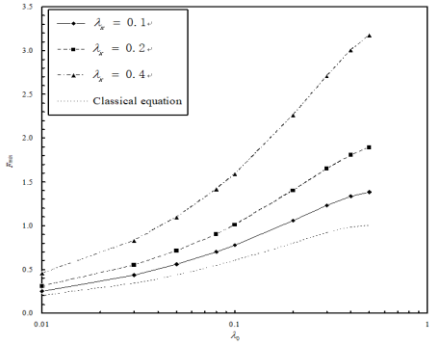

b) Medium interaction

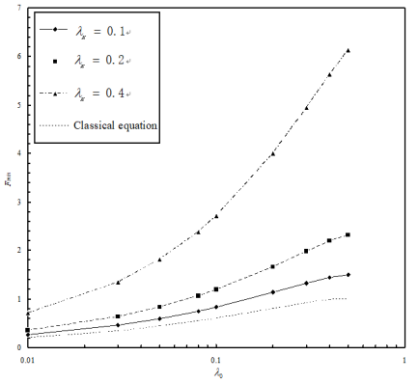

c) Strong interaction

Fig. 4 Continuation

5. Conclusions

The dimensionless flow resistances and the optimum values of R_1/R_0 of the nanoporous filtration membrane with double concentric cylindrical pores where the multiscale flow occurs are calculated from the developed multiscale scheme for widely varying operational parameter values when the liquid-pore wall interaction is respectively weak, medium and strong. The results show that when $\lambda_x \geq 1$, the flow resistance or flux of the membrane should be calculated from the multiscale approach owing to the adsorbed layer effect, as the classical calculation will be significantly erroneous. When the liquid-pore wall interaction is weak, the optimum value (i.e. $(R_1/R_0)_{opt}$)) of R_1/R_0 for the lowest flow resistance of the membrane can be calculated from the classical equation even for the membrane in the multiscale flow; However for medium and strong liquid-pore wall interactions, when $\lambda_x \geq 1$, the values of $(R_1/R_0)_{opt}$ should be calculated from the multiscale scheme as the classical calculation ignores the significant multiscale effect in this case and thus brings considerable errors.

References

1. **Ariono, D.; Aryanti, P. T. P.; Wardani, A. K.; Wenten, I. G.** 2018. Fouling characteristics of humic substances on tight polysulfone-based ultrafiltration membrane, Membrane Water Treatment 9: 353-361. https://doi.org/10.12989/mwt.2018.9.5.353.
2. **El-ghzizel, S.; Jalté, H.; Zeggar, H.; Zait, M.; Belhamidi, S.; Tiyal, F.; Hafsi, M.; Taky, M.; Elmidaoui, A.** 2019. Autopsy of nanofiltration membrane of a decentralized demineralization plant, Membrane Water Treatment 10(4): 277-286.

https://doi.org/0.12989/mwt.2019.10.4.277.
3. **Fissel, W. H.; Dubnisheva, A.; Eldridge, A. N.; Fleischman, A. J.; Zydney, A. L.; Roy, S.** 2009. High-performance silicon nanopore hemofiltration membranes, Journal of Membrane Science 326(1): 58-63. http://dx.doi.org/10.1016/j.memsci.2008.09.039.
4. **Jackson, E. A; Hillmyer, M. A.** 2010. Nanoporous membranes derived from block copolymers: From drug delivery to water filtration, ACS Nano 4(7): 3548-3553. http://dx.doi.org/10.1021/nn1014006.
5. **Jin, Y.; Choi, Y.; Song, K. G.; Kim, S.; Park, C.** 2019. Iron and manganese removal in direct anoxic nanofiltration for indirect potable reuse, Membrane Water Treatment 10(4): 299-305. https://doi.org/0.12989/mwt.2019.10.4.299.
6. **Jung, J.; Shin, B.; Park, K. Y.; Won, S.; Cho, J.** 2019. Pilot scale membrane separation of plating wastewater by nanofiltration and reverse osmosis, Membrane Water Treatment 10(3): 239-244. https://doi.org/10.12989/mwt.2019.10.3.239.
7. **Rashidi, H.; Meriam, N.; Sulaiman, N.; Hashim, N. A.; Bradford, L.; Asgharnejad, H.; Larijani, M.** 2020. Development of the ultra/nano filtration system for textile industry wastewater treatment, Membrane Water Treatment 11(5): 333-344. https://doi.org/10.12989/mwt.2020.11.5.333.
8. **Surwade, S. P.; Smirnov, S. N.; Vlassiouk, I. V.; Unocic, R. R.; Veith, G. M.; Dai, S.; Mahurin, S. M.** 2015. Water desalination using nanoporous single-layer grapheme, Nature Nanotechnology 10: 459-464. https://doi.org/10.1038/nnano.2015.37.
9. **Yang, S. Y.; Ryu, I.; Kim, H. Y.; Kim, J. K.; Jang, S. K.; Russell, T. P.** 2006. Nanoporous membranes with ultrahigh selectivity and flux for the filtration of viruses, Advanced Materials 18(6): 709-712. https://doi.org/10.1002/adma.200501500.
10. **Zhang, Y. B.** 2018. Optimum design for cylindrical-shaped nanoporous filtration membrane, International Communications in Heat and Mass Transfer 96: 130-138. https://doi.org/10.1016/j.icheatmasstransfer.2018.06.003.
11. **Baker, L. A.; Bird, S. P.;** 2008. Nanopores: A makeover for membranes, Nature Nanotech. 3(2): 73-74. http://dx.doi.org/10.1038/nnano.2008.13.
12. **Li, N.; Yu, S.; Harrell, C.; Martin, C. R.** 2004. Conical nanopore membranes: Preparation and transport properties, Analytical Chemistry 76(7): 2025-30. http://dx.doi.org/10.1021/ac035402e.
13. **Tiraferri, A.; Yip, N. Y.; Phillip, W. A.; Schiffman, J. D.; Elimelech M.** 2011. Relating performance of thin-film composite forward osmosis membranes to support layer formation and structure, Journal of Membrane Science 367(1): 340-352. http://dx.doi.org/10.1016/j.memsci.2010.11.014.
14. **Yip, N. Y.; Tiraferri, A.; Phillip, W. A.; Schiffman, J. D.; Elimelech, M.** 2010. High performance thin-film composite forward osmosis membrane, Environmental Science and Technology 44(10): 3812-3818. http://dx.doi.org/0.1021/es1002555.
15. **Bitsanis, I.; Magda, J. J.; Tirrell, M.; Davis, H. T.** 1987. Molecular dynamics of flow in micropores, Journal of Chemical Physics 87(3):1733-1750. http://dx.doi.org/10.1016/10.1063/1.453240.
16. **Somers, S. A.; Davis, H. T.** 1992. Microscopic dynamics of fluids confined between smooth and atomically structured solid surfaces. Journal of Chemical Physics 96 (7): 5389-5407. https://doi.org/10.1063/1.462724.
17. **Sun, J.; He, Y.; Tao, W. Q.** 2010. Scale effect on flow and thermal boundaries in micro-/nano- channel flow using molecular dynamics-continuum hybrid simulation method, International Journal for Numerical Methods in Engineering 81(2): 207-228. https://doi.org/10.1002/nme.2683.
18. **Yen, T. H.; Soong, C. Y.; Tzeng, P. Y.** 2007. Hybrid molecular dynamics-continuum simulation for nano/mesoscale channel flows, Microfluid Nanofluid 3: 665-675. https://doi.org/10.1007/s10404-007-0202-3.
19. **Tang, Z. P.; Zhang, Y. B.** 2022. Multiscale analysis of the performance of micro/nano porous filtration membranes with double concentric cylindrical pores: Part I-Analysis development, Mechanika 28(3): 211-216. http://dx.doi.org/10.5755/j02.mech.30507.

Z. Tang, Y. Zhang

MULTISCALE ANALYSIS OF THE PERFORMANCE OF MICRO/NANO POROUS FILTRATION MEMBRANES WITH DOUBLE CONCENTRIC CYLINDRICAL PORES: PART II-OPTIMIZATION RESULTS

S u m m a r y

The multiscale calculation results for the values of the optimized parameters are presented for the micro/nano porous filtration membranes with double concentric cylindrical pores where multiscale flows occur. For a weak liquid-pore wall interaction, the optimum ratio of the radius of the bigger pore to the radius of the smaller pore (i.e. the filtration pore) can be calculated from the classical equation, however the corresponding lowest flow resistance of the membrane should still be calculated from the multiscale analysis owing to the adsorbed layer effect when the ratio λ_x of the thickness of the adsorbed layer to the radius of the smaller pore is greater than 0.1. For medium and strong liquid-pore wall interactions, the optimum ratios of the pore radii should be calculated from the multiscale analysis, and the corresponding lowest flow resistances of the membrane are much higher than the classical calculation showing the significant effect of the adsorbed layer when $\lambda_x \geq 0.1$.

Keywords: adsorbed layer, filtration, multiscale flow, membrane, nanopore, optimization.

Received January 21, 2022
Accepted June 14, 2022